Journal of Information Engineering and Applications
ISSN 2224-5782 (print) ISSN 2225-0506 (online)
Vol 2, No.10, 2012

Modeling and Simulation of a Photovoltaic Powered Vapour Compression Refrigeration System

Mba E.F., Chukwuneke J.L.*, Achebe C.H., Okolie P.C.

Department of Mechanical Engineering, Nnamdi Azikiwe University, P.M.B 5025 Awka, Anambra Nigeria

*E-mail of the corresponding author: jl.chukwuneke@unizik.edu.ng

Abstract

This paper presents a mathematical model of a solar vapour compression refrigeration system. The system consists of a D.C. vapour compression refrigerator, a controller that prevents the battery from being over charged or deep-discharged, a D.C inverter which converts direct current from the solar photovoltaic panel or the battery into alternating current that can be fed to the refrigerator's compressor, a battery to store and supply energy when the sun is not available and a photovoltaic (PV) generator which supplies power to the refrigerator and charges the battery with excess energy. The different components of the system are modeled, the output from one component becoming the input to the next component. The significance of the resulting photovoltaic powered vapour compression refrigeration is to develop a computer model and simulation for a photovoltaic powered refrigeration system and MatLab is used to simulate the system performance. The simulation gives the system relationship between the freezer temperatures that can be attained and incident solar radiation on the solar PV panel using different solar panels. The battery size required to run the system for a maximum period of 12 hours was derived. It was determined that as the system voltage increased, the battery size required to run the system decreased. The current-voltage and power-voltage characteristics of the KC65T PV panel by Kyocera were studied. It was observed that the open circuit voltage (voltage produced when the PV panel's terminals, shorting it out) increased linearly. This behavior indeed showed that a PV cell behaves more like a current source than a voltage source. It was also observed that the power at MPP (maximum power point) increased with increasing solar insolation while the V_{mp} (Voltage at MPP) remained constant at 14.2 volts irrespective of the level of incident solar insolation. This finding suggested that for any particular solar PV panel model, maximum power can be obtained at a particular voltage (14.2 volts in this case), when working at any given solar insolation level. The current at maximum power, I_{mp} was observed to increase with increasing solar insolation.

Keywords: photovoltaic system, vapour compression refrigeration, inverter, solar photovoltaic panel, solar energy and insolation, solar cells and battery.

1. Introduction

Solar irradiance is a key driving force of the earth. It is also ultimately the source of all energy supplies except for nuclear energy. Current and fossil biomass grew by photo-synthesis. Hydroelectric, wind and wave energies are linked to climate, which is also driven by the sun through uneven heating on the earth. Direct conversion of solar irradiance through solar energy systems is obviously linked to the sun as well.

1.1. The Basis for Considering Solar Energy

There are several important reasons for considering solar energy as an energy resource to meet the needs of developing countries. First, the solar energy received by earth is more than 10,000 times the current use of fossil fuels and nuclear energy combined. This means that harnessing such a large energy source has the potential to replace a significant amount of carbon based fuels thus, reducing the amount of carbon dioxide and other green house emissions. Secondly, energy is a critical need of many countries but they do not have widely distributed readily available supplies of conventional energy resources. Thirdly, most of the developing countries are characterized by arid climates, dispersed and inaccessible populations and a lack of investment capital and are thus faced with practically inseparable obstacles to the provision of energy by conventional means, for example, by electrification. In contrast to this, solar energy is readily available and is already distributed to the potential users.

Fourthly, most of the countries called developing are in or adjacent to the tropics and have good solar radiation available.

1.2. Objectives

The task of this paper is to develop a mathematical model for a photovoltaic powered vapor compression refrigeration system. A relationship between the solar radiation intensity and the temperature attained in the refrigerator will be sought. The components of the stand alone system described in this paper are a PV array, a charge controller, a battery, an inverter and a vapor compression refrigerator. Fig.1 shows the system configuration.

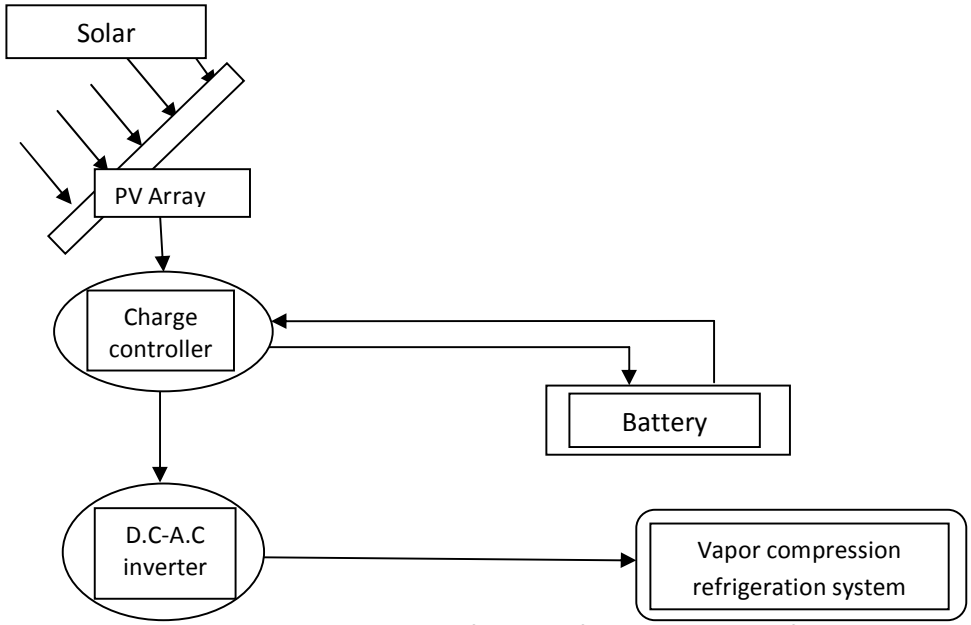

Figure1. System configuration for a PV powered refrigerator

2. Systems Descriptions

2.1 Photovoltaic (PV) Arrays

A basic solar PV panel consists of connected PV cells, which contain a semiconductor material covered by protective glass connected to a load. When sunlight hits the semiconductor, electrons become excited. These excited electrons are separated by an internal field inherent in the semiconductor and collected into an external circuit generating electricity. Several connected PV cells form a PV module; connected modules form a PV array.

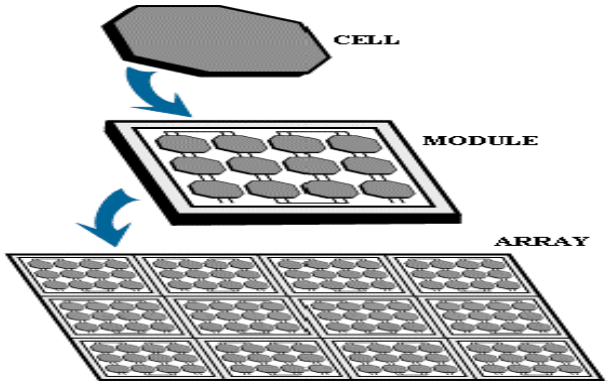

Figure2. A solar photovoltaic array

The necessary size of the array for a particular load depends primarily on the meteorological conditions. A PV array delivers energy depending on the incident solar radiation. This work describes a mathematical model for a PV module. The information on which this model is based can be found in (Eckstein, 1990; Duffle et al, 1991).

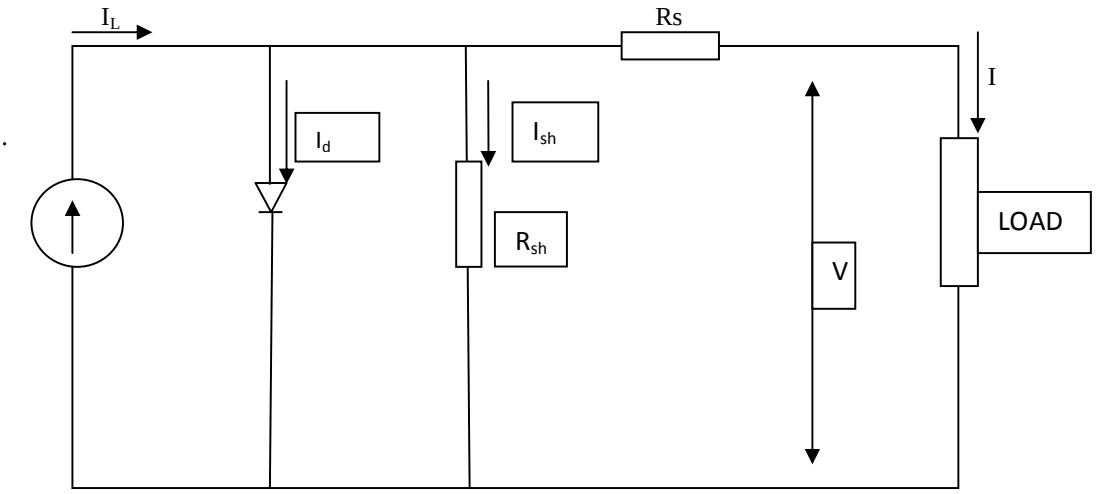

Figure3. Equivalent electrical circuit for a PV generator

The light current, I_l, is generated from the PV array and is proportional to the incident radiation. The diode describes the semiconductor behavior of the PV cells. The current through the diode, I_d, is the loss current through the junction of the cell. The shunt resistance, R_{sh}, accounts for leakage losses at the outer edges of the cell and is usually very large, and often neglected. In this model, R_{sh} is assumed to be infinite. The series resistance, R_s, accounts for the resistances at the connections between cell and contact grid.

2.1.1 Governing equations and I-V characteristics of the PV module

Applying Kirchhoff's law to the circuit, we have that: $$I = I_L - I_d - I_{sh} \quad (1)$$

Where; $\mathbf{I_L}$ is the light current, $\mathbf{I_d}$ is the current through the diode, I_{sh} is the current through the shunt resistance.

Current through the diode can be expressed as: $$I_d = I_o\left\{\exp\left(\frac{V+IR_s}{\gamma}\right)-1\right\} \quad (2)$$

And current through the shunt resistance can be expressed as: $$I_{sh} = \frac{V+IR_s}{R_{sh}} \quad (3)$$

Applying these in eqn. 1, we have; $$I = I_L - I_o\left\{\exp\left(\frac{V+IR_s}{\gamma}\right)-1\right\} - \frac{V+IR_s}{R_{sh}} \quad (4)$$

Where; $\mathbf{I_o}$ is the diode reverse saturation current, $\mathbf{V}$ is the output voltage, $\mathbf{R_s}$ is the series resistance, $\mathbf{R_{sh}}$ is the shunt resistance, $\boldsymbol{\gamma}$ is a curve fitting parameter.

When the voltage, V is zero, short circuit conditions exist. The current at this point is called short circuit current, $\mathbf{I_{sc}}$. If the load resistance is infinite, the current is zero; the voltage is at its maximum. This voltage is called open circuit voltage, $\mathbf{V_{oc}}$. The voltage at the point where the power supplied reaches its maximum is denoted as $\mathbf{V_{mp}}$ and the current at this point as $\mathbf{I_{mp}}$.

The manufacturers of PV modules usually provide measured values of $\mathbf{V_{oc}}$, $\mathbf{I_{sc}}$, $\mathbf{V_{mp}}$ and $\mathbf{I_{mp}}$ at reference conditions. The reference conditions usually are at an incident solar radiation of 1000W/m^2 and an ambient temperature of 25^{o}C. With these measured values, the four parameters $\mathbf{I_L}$, $\mathbf{I_o}$, $\mathbf{R_s}$ and $\boldsymbol{\gamma}$ can be evaluated. $\mathbf{R_{sh}}$ is assumed to be infinite and therefore is neglected. At short circuit conditions, the diode current, I_d is very small and can be neglected. It then follows that the light current, I_L is equal to the short circuit current, $\mathbf{I_{sc}}$. $I_L = I_{sc}$ (5)

Under open circuit conditions, the load current, *I*, is zero. The light current is equal to the current through the diode. We then have from eqn. 2 that:

$$I_o = I_L \exp\left(-\frac{V_{oc}}{\gamma}\right) \quad (6)$$

The "1" in eqn. 2 is neglected because it is small when compared to the exponential term.

The series resistance can be calculated from:

$$R_s = \frac{\gamma \ln\left(1 - \frac{I_{mp}}{Isc}\right) - V_{mp} + V_{oc}}{I_{mp}} \quad (7)$$

In addition to the four values provided by the PV modules manufacturers, they also provide the cell temperature at reference conditions and the temperature coefficients for the short circuit current, μI_{sc} and the open circuit voltage, μV_{oc}. With these coefficients known, we can now decipher the values of the curve fitting parameter at reference conditions. The relationship is shown as:

$$\gamma_{ref} = \frac{\mu V_{oc} T_{cref} - V_{oc} + \varepsilon N_s}{\left(\frac{\mu I_{sc} T_{cref}}{I_{Lre}}\right) - 3} \quad (8)$$

Where; ε is the band gap energy (1.12 eV for silicon), N_s is the number of cells in the PV array, γ_{ref} is the curve fitting parameter at reference conditions, T_{cref} is the cell temperature at reference conditions, I_{Lref} is the light current at reference conditions, μI_{sc} is the temperature coefficients for the short circuit current, μV_{oc} is the temperature coefficients for the open circuit voltage.

With eqn. 8, (Townsend, 1989) showed that the following equations are valid for PV modules:

$$\frac{\gamma}{\gamma_{ref}} = \frac{T_{cref}}{T_c} \quad (9)$$

$$I_L = \left(\frac{G_T}{G_{Tref}}\right)\left\{I_{sc} + \mu I_{sc}\left(T_c - T_{cref}\right)\right\} \quad (10)$$

$$\frac{I_o}{I_{oref}} = \left(\frac{T_c}{T_{cref}}\right)^3 \exp\left\{\varepsilon N_s\left(1 - \frac{T_{cref}}{T_c}\right)\right\} \quad (11)$$

Where; G_T is the solar insolation (W/m^2), G_{Tref} is the solar insolation at reference conditions (W/m^2), T_c is the PV cell temperature (^{o}C), I_{oref} is the diode reverse saturation current at reference conditions (A).

2.1.2. Efficiency of a Solar Panel

The efficiency of a solar panel, η is defined as the ratio of power output (useful power), Q_s in KW to the product of the solar panel surface area, A_s (m^2) and the direct insolation on the solar panel, G_T(KW/m^2) (Kim et al, 2008; Zekai, 2008). The value of G_T depends on meteorological conditions. Mathematically, the efficiency of a solar panel can be expressed as:

$$\eta = \frac{Q_s}{G_T A_s} \quad (12)$$

2.1.3. Influence of the Solar Cell Temperature

The solar energy that is absorbed by the module is converted into thermal energy and electrical energy. The electrical behavior of the PV module has been described in the previous sections. We now want to analyze the influence of the solar cell temperature on the I-V characteristics. To determine the cell temperature of a PV module, an energy balance is made (Iloeje, 1977; Zekai, 2008):

Power absorbed by the solar PV panel is;

$$Q_p = G_T A_s \alpha \tau \quad (13)$$

Where; Q_p = Absorbed power (W), G_T = Total insolation (KW/ m^2), A_s = Area of PV panel, α = absorptance factor of the collector plate, τ = Transmission factor of the solar panel

Power loss in form of heat is;

$$Q_L = U A_s \left(T_c - T_a\right) \quad (14)$$

Where; Q_L = Power loss from the collector plate, U = collector U-value, T_c = Temperature of collector plate, T_a = Ambient air temperature

Hence, useful power is given as $Q_s = Q_p - Q_L$;

$$Q_s = G_T A_s \alpha \tau - U A_s \left(T_c - T_a\right) \quad (15)$$

From eqn. 12 it could be derived that;

$$Q_s = \eta G_T A_s \quad (16)$$

Equating [eqn. 15] and [eqn. 16], we get;

$$\eta G_T A_s = G_T A_s \alpha \tau - U A_s \left(T_c - T_a\right) \quad (17)$$

Assuming unit area, we have; $\eta G_T = G_T \alpha \tau - U(T_c - T_a)$ (18)

From eqn. 18 we have; $T_c = T_a + (G_T \tau\propto/U)(1 - \eta/\tau\propto)$ (19)

The ratio $(\tau \propto/U)$ is assumed to be constant. To determine its value, the nominal operating cell temperature (NOCT) is measured. The NOCT conditions are an incident solar radiation of 800 W/m^2, a wind speed of 1 m/s and an ambient temperature of 20^{o}C. The measurement is made under no load conditions.

The measurement is made under no load conditions. In this case, the efficiency,η, is zero. Eqn. 19 then becomes: $T_c = T_a + (G_T \tau\propto/U)$ and making $\tau \propto/U$ subject, we have; $\frac{\tau\alpha}{U} = \frac{T_c - T_a}{G_T}$

Applying the NOCT conditions, we have that; $\frac{\tau\alpha}{U} = \frac{T_{c,noct} - T_{a,noct}}{G_{Tnoct}}$ (20)

Where; $T_{c,noct}$ = 319K, $T_{a,noct}$ = 293K, $G_{T,noct}$ = 800W/ m^2. Substituting these values in equation 20; $\frac{\tau\alpha}{U}$ =0.0325K- m^2 /W, $\tau \propto$ = 0.9 {Used by all solar panel manufacturers} (Eckstein, 1990).

Substituting these values into equation 19; $T_c = T_a + (0.0325G_T)(1 - \eta/0.9)$ (21)

Eqn. 21 shows a relationship between the cell temperature, T_c, the ambient temperature, T_a, the insolation level, G_T and the efficiency of the solar panel, η. It then follows that we can actually calculate the cell temperature at any given ambient temperature, insolation level and solar panel efficiency. Once the cell temperature, T_c has been deciphered, the value is used to solve for current and voltage and the I-V and P-V characteristics are found with a cell temperature that depends on the ambient temperature.

2.2. Battery Storage

The importance of a power storage unit in any solar power generation system cannot be overemphasized. As we all know, the sun's supply of energy is epileptic and so any system designed to be powered by the sun must have an alternative source of power to run the system, when the sun's supply of power becomes low or unavailable. The battery provides this storage source. It stores electrical energy when the solar insolation is enough to power the load and this stored energy is used to run the system when the solar panel cannot produce enough power to carry the load.

This paper does not consider thermal effects and battery aging (i.e. the number of charging-discharging cycles the battery has undergone). Also, self-discharge is neglected. In this paper, we are more concerned about the charging efficiency of the battery, η_{ch}.This charging efficiency is assumed to be constant and takes into account that some energy is wasted in producing gas. The energy losses are given by (Zekai, 2008, Kribus, 2002);

$$P_{loss} = (1 - \eta_{ch})P \quad (22)$$

Where; P is the input energy/power. The power produced by the battery is given as: $P_{bat} = P - P_{loss}$ (23)

Substituting the value of P_{loss} of eqn. 22 into eqn. 23; $P_{bat} = P - (1 - \eta_{ch})P$. Hence; $P_{bat} = \eta_{ch} P$ (24)

2.2.1. Charge Controllers

A charge control is needed when using a battery for energy storage in PV systems. The battery must be protected from overcharge and from deep discharge or damage to the battery may result. In this model, the parallel controller is used. The system configuration of the PV system with the parallel type charge controller is shown in Fig. 4.

The parallel controller consists of the overcharge and the deep discharge protection. When enough energy is provided from the PV array, and the battery reaches its maximum state of charge, the relay for the overcharge protection opens. The battery cannot be charged any more. Assuming no self discharge, the state of charge stays constant. The load is supplied from the PV array, when possible. If the state of charge is at its minimum and the PV current cannot meet the load, the relay for the deep discharge protection opens and the load is disconnected from the system. The PV array charges the battery. If the PV current can meet the load again, the deep discharge relay closes and the load is reconnected. The battery is charged if the PV current is in excess of that needed to supply the load.

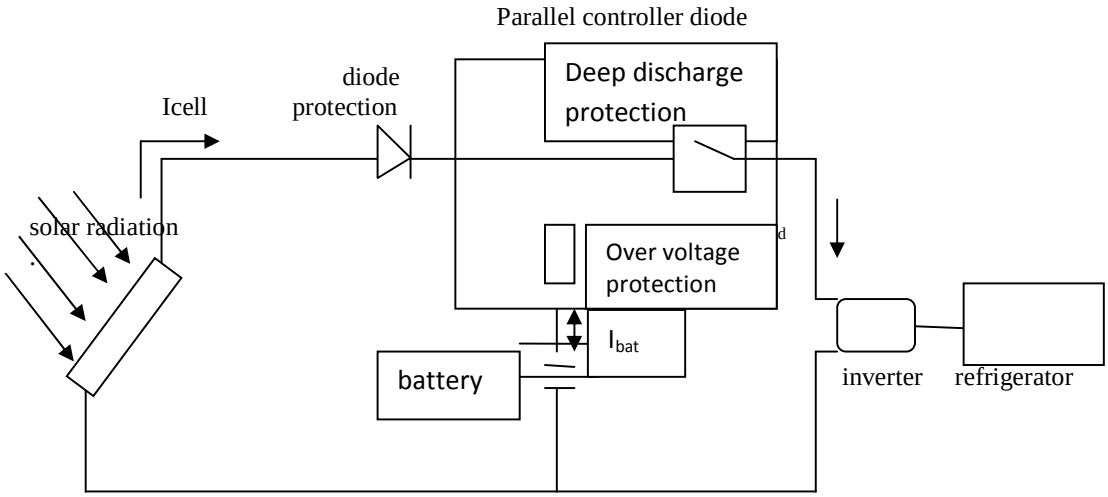

Figure 4. PV system configuration including a parallel controller

2.3. The Inverter

Inverters are power devices, which convert direct current, DC (typically at low voltage) into alternating current, AC as required by conventional appliances. There are generally two types of photovoltaic inverters available: the stand alone inverters and the grid-connected inverters.

2.3.1. Stand Alone Inverters

Stand alone or battery supplied inverters are demand-driven; they provide any power or current up to the rating of the inverter and assuming that there is enough energy in the battery. These inverters are being used increasingly to operate household appliances and other 'normal' 230V equipment.

2.3.2. Grid-Connected Inverters

Grid-connected inverters are supply-driven, they provide all the power supplied from a D.C source to the grid or mains. Therefore, in grid-connected systems, the solar inverter is the connecting link between the solar generator and the A.C grid. In this thesis, we are concerned with the stand alone inverters.

2.3.3. Operation of the Inverter

The basic theory of operation behind an inverter is as follow: See Figure5.

The top transistor switch closes and causes current to flow from the battery negative through the transformer primary to the battery positive. This induces a voltage in the secondary side of the transformer that is equal to the battery voltage times the turn's ratio of the transformer. After a period of approximately 8mins, the switches flip-flop, the top switch opens and the bottom switch closes allowing current to flow in the opposite direction.

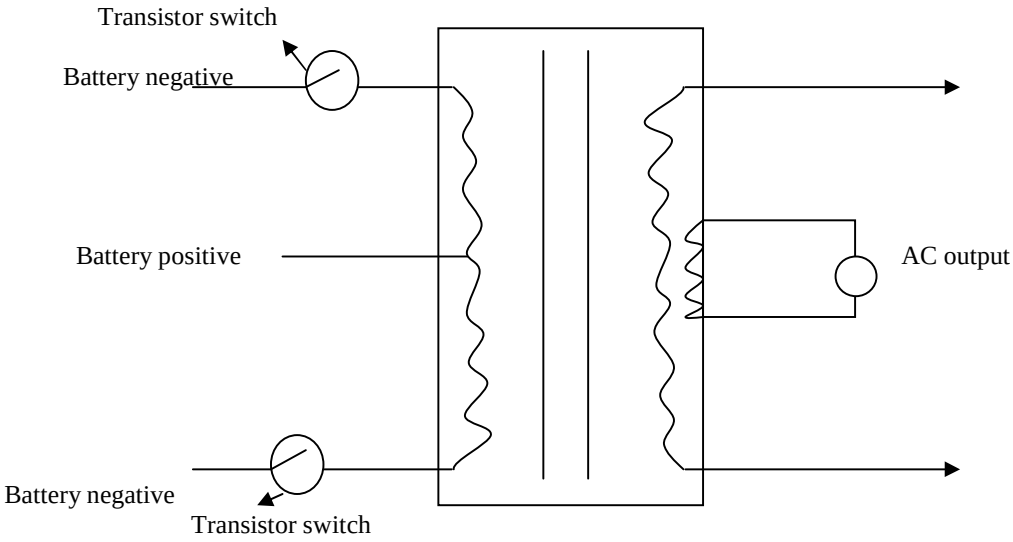

Figure5. Schematic of a DC-AC inverter

2.3.4. The Efficiency of an Inverter

The efficiency of the inverter is the most important aspect of the inverter as far as this thesis is concerned, because it will give us the AC power output we are going to get for every DC power input into the inverter.

The efficiency of an inverter can be given as (Zekai, 2008): $\eta_{inv} = (P_{out}/P_{in})100$ (25)

Where; P_{out} is the output power from the inverter, P_{in} is the input power to the inverter.

It then follows that with this efficiency known, one can decipher the power input required to achieve any needed power output simply by applying equation 25.

2.4. The Refrigeration System

Here we describe the commonly used vapor compression refrigeration cycle and its components. The basic vapor compression system comprises of a compressor, condenser, throttling valve and the evaporator as shown in the diagram below:

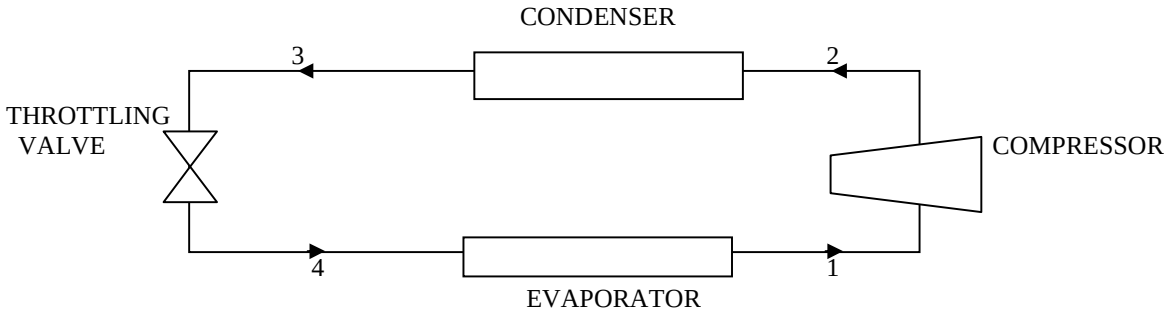

Figure6. A basic Vapor Compression Refrigeration Cycle

In this paper, the refrigerator is modeled with refrigerant R134a because it has no effect on the ozone layer and since it is a global need to reduce the emission of dangerous gases into the atmosphere, it is a right choice. The pressure-enthalpy (P-h) and temperature-entropy (T-s) diagrams describing the basic vapor compression cycle are shown below:

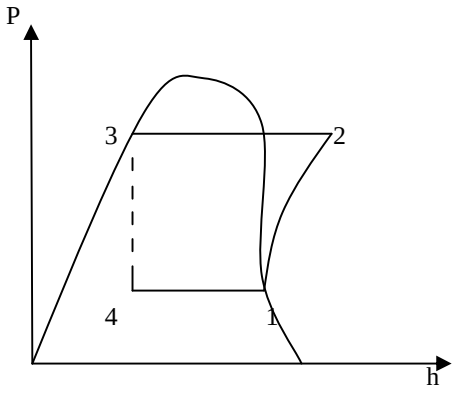

Figure7a. Pressure-Enthalpy Diagram for an Ideal Vapor Compression Cycle

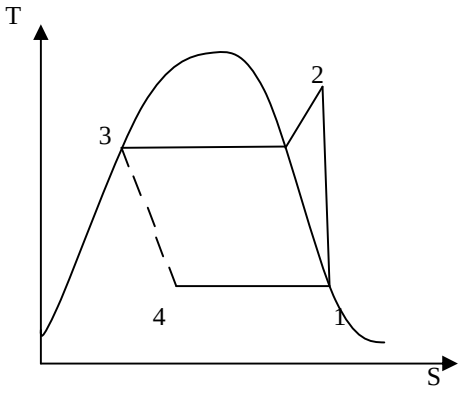

Figure7b. Temperature-Enthalpy Diagram for an Ideal Vapor Compression Cycle

2.4.1. Refrigeration Cycle Description

The ideal cycle considers heat transfer in the condenser and evaporator without pressure losses, a reversible adiabatic compressor and an adiabatic expansion valve, connected through piping that has neither pressure loss nor heat transfer with the surroundings. The refrigerant leaves the evaporator at point 1 as a low pressure, low temperature, and saturated vapor and enters the compressor where it is compressed reversibly and adiabatically (or isentropically). At point 2, it leaves the compressor as a high temperature, high pressure, and super-heated vapor and enters the condenser. In the condenser, the refrigerant is first de-superheated and then condensed at a constant pressure. At point 3, it leaves the condenser as a high pressure, medium temperature, saturated liquid and enters the expansion valve, where it expands irreversibly and adiabatically (constant enthalpy). At point 4, the refrigerant leaves the expansion valve as a low-quality vapor and enters the evaporator, where it is evaporated reversibly at constant pressure to the saturation state of point 1.

2.4.2. Governing Equations

The energy equation for a steady-flow process, (McConkey, 2003; Shan, 2000): $\frac{V_1^2}{2g} + Z_1 + h_1 + q = \frac{V_2^2}{2g} + Z_2 + h_2 + W$

Where; $V^2/2g$ is the kinetic energy term, Z is the potential energy term, h is the enthalpy, W is work, q is heat transfer.

In the case of a refrigeration system, the changes in kinetic and potential energies are neglected, thus reducing the energy equation to: $h_1 + q = h_2 + W$ (26)

2.4.3. The Compressor (Process: 1-2)

Here, the refrigerant is compressed reversibly and adiabatically (i.e. no heat transfer component). Therefore, energy equation reduces to: $h_1 = h_2 + W$; $W = h_1 - h_2$; $W_{in} = h_2 - h_1$, Where; W_{in} is the power input to the compressor for unit mass flow rate of refrigerant, h_1 is the enthalpy of the refrigerant at point 1, h_2 is the enthalpy of the refrigerant at point 2. For a refrigerant mass flow rate "*m*"; $mW_{in} = m(h_2 - h_1)$; $P_{in} = m(h_2 - h_1)$ (27)

The refrigerant mass flow rate can be estimated from eqn. 27 with: $$m=\frac{P_{in}}{h_2 - h_1} \quad (28)$$

Where P_{in} is the compressor power input.

2.4.4. The Condenser (Process: 2-3)

In the condenser, heat is rejected to the surroundings and there is no work term (W = 0), the energy equation then reduces to: $q = h_3 - h_2$; $$Q_{rej} = m(h_2 - h_3) \quad (29)$$

Where; Q_{rej} is the rate at which heat is rejected from the condenser to the ambient, h_3 is the enthalpy of the refrigerant at point 3.

2.4.5. The Throttling Valve (Process: 3-4)

From State 3 to 4 the liquid flows through the throttling valve, where it undergoes an adiabatic expansion (constant enthalpy). Hence, we now have that: $$h_3=h_4 \quad (30)$$

Where; h_4 is the enthalpy of the refrigerant at point 4.

2.4.6. The Evaporator (Process: 4-1)

From state 4 to 1, the refrigerant flows through the evaporator, where it absorbs heat from the contents of the freezer. In this case there is no work done and the energy equation reduces to: $q = h_1 - h_4$

$$CAP = m(h_1 - h_4) \quad (31)$$

Where CAP is the heat transfer rate into the evaporator also known as the Refrigerating Capacity of the plant. The CAP is also expressed as the overall heat transfer coefficient area product times the temperature difference between refrigerant, and freezer. $$CAP = UA_{ev}(T_{fr} - T_{ev}) \quad (32)$$

Where; UA_{ev} is the overall heat transfer coefficient area product of the evaporator, T_{fr} and T_{ev} are the temperatures for freezer and the refrigerant in the evaporator respectively.

3. System Analysis

In this section, the relationships between the input and output of every component were discovered; the output from one component becomes the input to the next component. The analysis is done using different photovoltaic panel models. The information on these photovoltaic panels can be found in (BP Solar Corporation, 2008; Kyocera Solar, Inc., 2009; BJ Power Co. Ltd, 2009) and are summarized in table 1.

Table 1: Summary of specifications for the PV panel models used in this paper

PV PANEL	**V_{mp}(V)**	**I_{mp}(A)**	**V_{oc}(V)**	**I_{sc}(A)**	μV_{oc}(V/K)	μI_{sc}(A/K)	**N**	η(%)
BP4170	34.7	4.9	44	5.4	-0.36	0.065	60	13.2
BP3220	29	7.6	36.2	8.4	-0.36	0.065	60	13.2
BJP-230MA	36	4.72	43.9	5.10	-0.16	0.065	60	14.2
BJP-180MA	36.1	5	44.2	5.3	-0.16	0.065	60	14.2
KC65TS	17.4	3.75	21.7	3.99	-0.0821	0.00212	36	13.2

3.1. The Photovoltaic System Analysis

We now analyze the photovoltaic panel in order to get a relationship between the solar radiation (input) and power produced by the solar panel (output).

From eqn. 4 and neglecting Rsh: $$I = I_L - I_o\left\{\exp\left(\frac{V+IR_s}{\gamma}\right)-1\right\} \quad (33)$$

Eqn. 33 is a transcendental equation and was solved using MATLAB and the value of **I** was found to be:

$$I = I_L R_s - \frac{\gamma \mathbf{W}\left\{R_s I_o/\gamma \exp\left(\frac{V+I_L R_s+R_s I_o}{\gamma}\right)+R_s I_o\right\}}{R_s} \quad (34)$$

Where; **W** represents the Lambert W-function of the quantity in parentheses. Substituting eqn. 10 into eqn. 34:

$$I=\left(\frac{G_T}{G_{Tref}}\right)\{I_{sc}+\mu I_{sc}(T_c - T_{cref})\}R_s - \frac{\gamma W\left\{R_s I_o/\gamma \exp\left(\frac{V+\left(\frac{G_T}{G_{Tref}}\right)\{I_{sc}+\mu I_{sc}(T_c - T_{cref})\}R_s+R_s I_o}{\gamma}\right)+R_s I_o\right\}}{R_s} \quad (35)$$

Since power is given as: $Power = current \times voltage = IV$, the power developed by the solar panel, P_{sol} is then given as: $$P_{sol} = IV \quad (36)$$

Table 1 show the values of $\mathbf{V_{mp}}$, $\mathbf{I_{mp}}$, $\mathbf{V_{oc}}$, $\mathbf{I_{sc}}$, $\boldsymbol{\mu V_{oc}}$, $\boldsymbol{\mu I_{sc}}$, **N** and η used in the calculation. With eqn. 6, the current-voltage characteristics of a particular PV panel can be obtained for different insolation levels at any cell temperature, T_c. The values of I_o, T_c, R_s and γ can be obtain from eqns. 3, 21, 7 and 1 respectively. Figs. 8 - 11 below show the I-V characteristics of the KC65T solar panel by Kyocera.

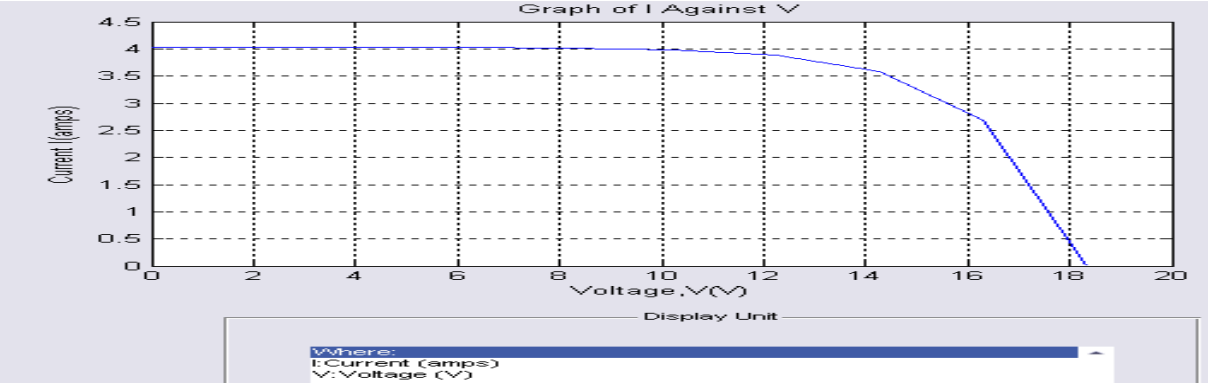

Fig.ure8. I-V curve for KC65T by Kyocera at a solar insolation level of 1000W/m^2

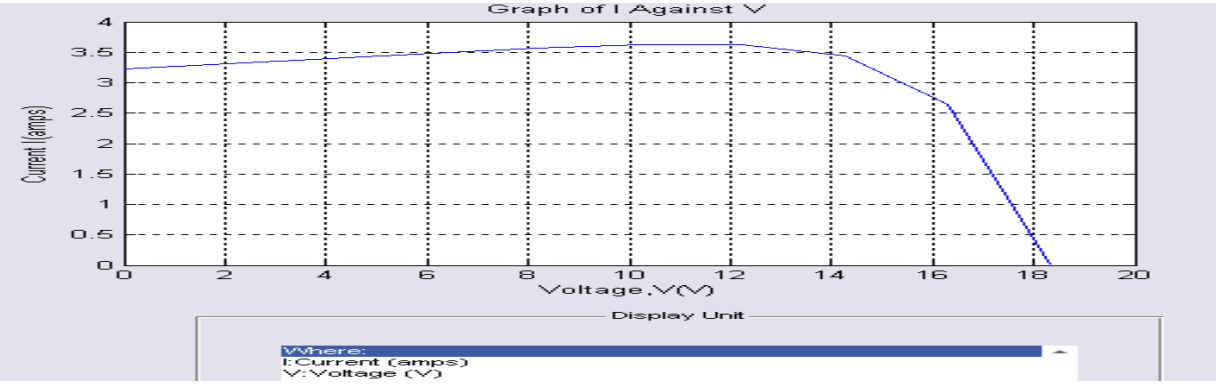

Fig.ure9. I-V curve for KC65T by Kyocera at a solar insolation level of 800 W/m^2

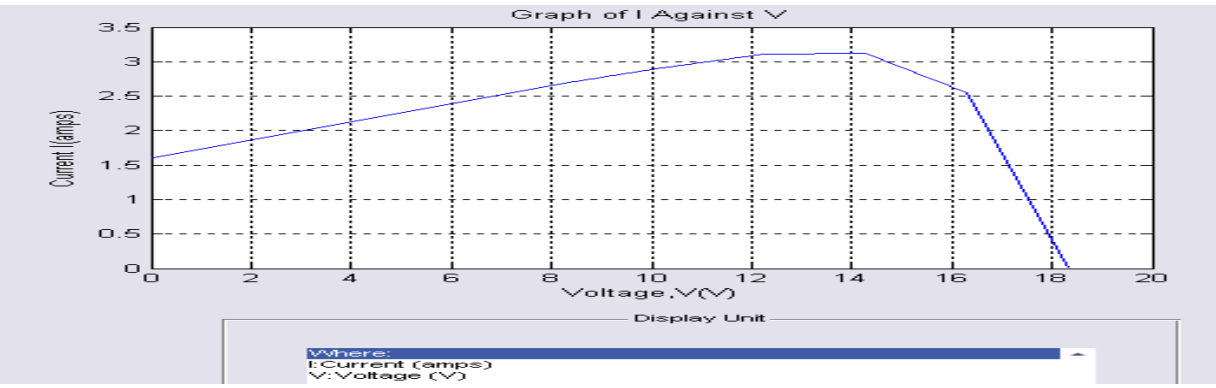

Figure10. I-V curve for KC65T by Kyocera at a solar insolation level of 400 W/m^2

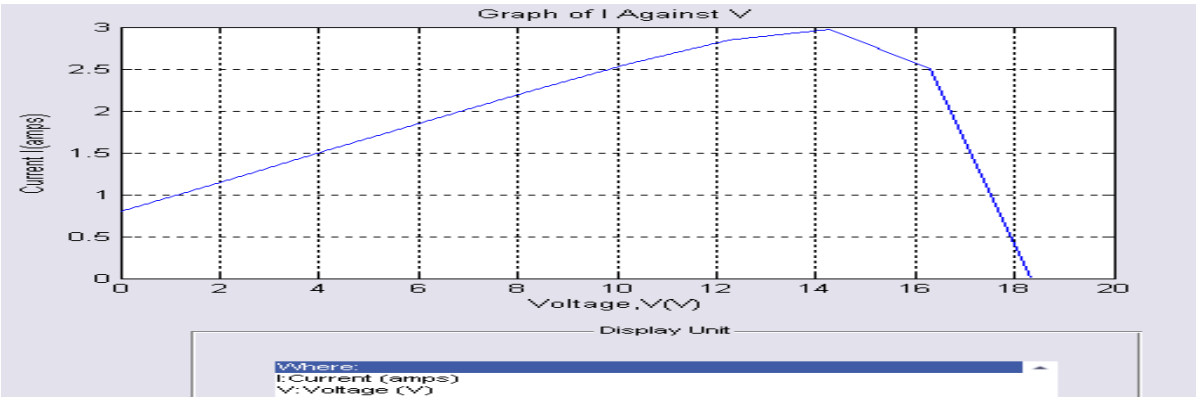

Figure11. I-V curve for KC65T by Kyocera at a solar insolation level of 200 W/m^2

Figs. 8 – 11 are very important curves which show that as the load current increases, the output voltage decreases in a non-linear fashion. Note the point at which each curve intersects the vertical axis (i.e. at V = 0). This is known as the short circuit condition, and it defines how the cell operates if a wire is connected between its terminals, shorting it out. The current flow here is known as the short circuit current, **Isc**. Because there is no voltage, the cell delivers no power at this point. Also, note the point at which each curve intersects the horizontal axis. This defines how the cell operates if it is not connected to any load. This is known as the open circuit condition, and the voltage produced is known as the open circuit voltage, **Voc**. Because the current is zero, no power is delivered at this point. Table 2 below shows a summary of the values of $\mathbf{I_{sc}}$ and $\mathbf{V_{oc}}$ at different solar insolation.

Table 2: Summary of the values of I_{sc} and V_{oc} at different solar insolation

G_T	I_{sc}	V_{oc}
1000	4.05	18.2
800	3.2	18.2
400	1.65	18.2
200	0.8	18.2

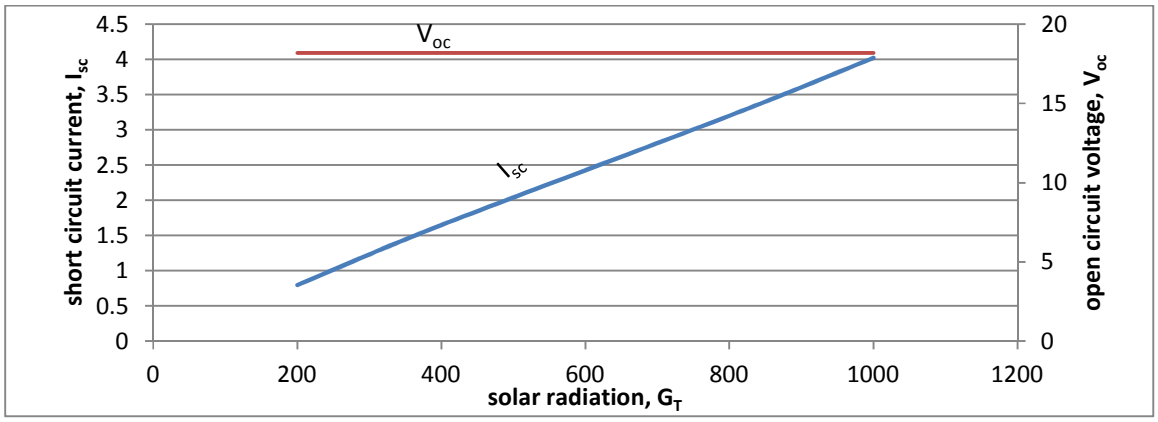

Figure12. The effect of varying G_T on I_{sc} and V_{oc}

The effect of varying solar insolation on I_{sc} and V_{oc} is seen on fig. 12 above. A close observation of fig. 12 shows that the current produced is proportional to the incident solar insolation impinging on the PV panel (i.e. the higher the solar insolation), the greater the amount of current produced while the voltage capability of the cell is almost constant. It can be seen that the Open circuit voltage remains constant with increasing solar insolation while the short circuit current increases linearly. This behavior indeed enunciates that a PV cell behaves more like a current source than a voltage source. Here it is note-worthy to see that a PV cell generates both current and voltage and acts as a photovoltaic generator.

For each point on the graph, the voltage and current can be multiplied to calculate power. From eqn. 36, substituting the value of **I** from eqn. 35, then;

$$Psol = \left\{ \left(\frac{G_T}{G_{Tref}}\right)\{I_{sc} + \mu I_{sc}(T_c - T_{cref})\}R_s - \frac{\gamma \mathbf{W}\left\{R_s I_o / \gamma \exp\left(\frac{V + \left(\frac{G_T}{G_{Tref}}\right)\{I_{sc} + \mu I_{sc}(T_c - T_{cref})\}R_s + R_s I_o}{\gamma}\right)\right\} + R_s I_o}{R_s} \right\} V \quad (37)$$

From table 1, the values of $\mathbf{V_{mp}}$, $\mathbf{I_{mp}}$, $\mathbf{V_{oc}}$, $\mathbf{I_{sc}}$, μV_{oc}, μI_{sc}, **N** and η used in the calculations can be found. With eqn. 37, the power-voltage characteristics of a particular PV panel can be obtained for different insolation levels at any cell temperature, T_c. The values of I_o, T_c, R_s and γ can be calculated from eqns. 11, 21, 7 and 9 respectively. Figs. 4.6 - 4.9 show the power-voltage characteristics of the KC65T solar panel by Kyocera.

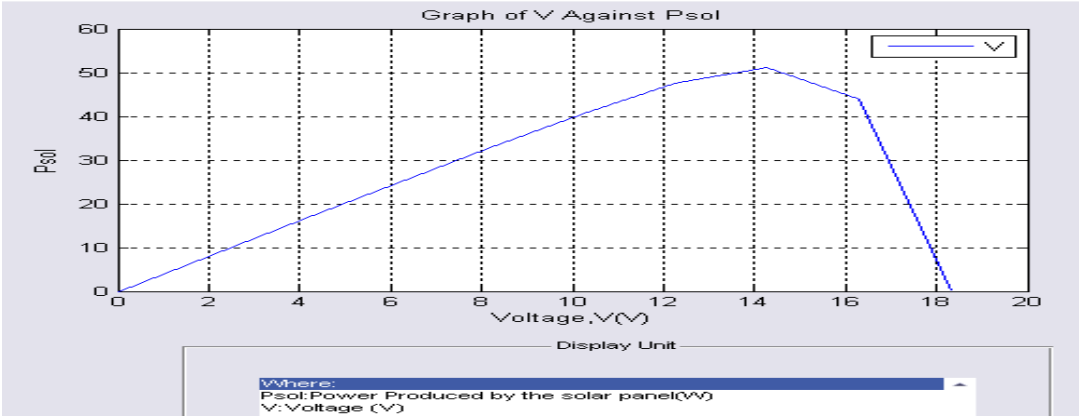

Figure13. Psol-V curve for the KC65T by Kyocera at an incident solar radiation of 1000W/m^2

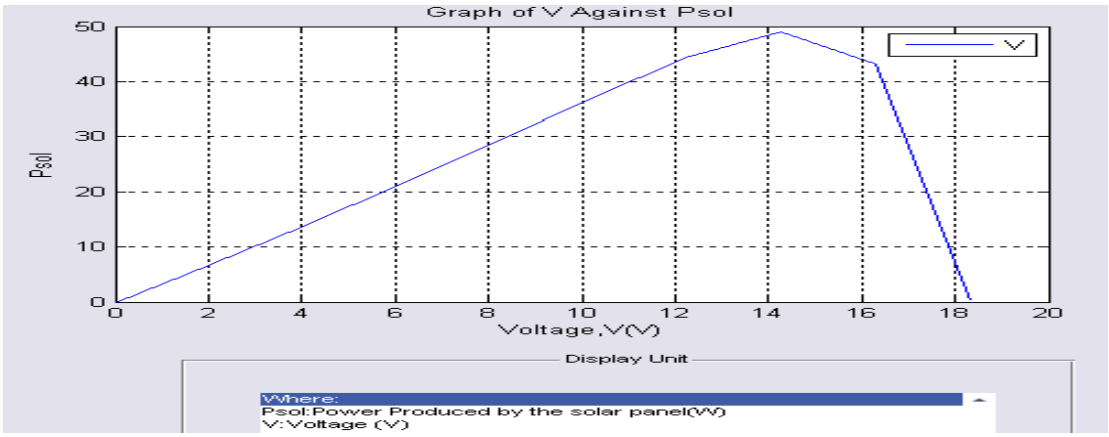

Figure14. Psol-V curve for the KC65T by Kyocera at an incident solar radiation of 800W/m^2

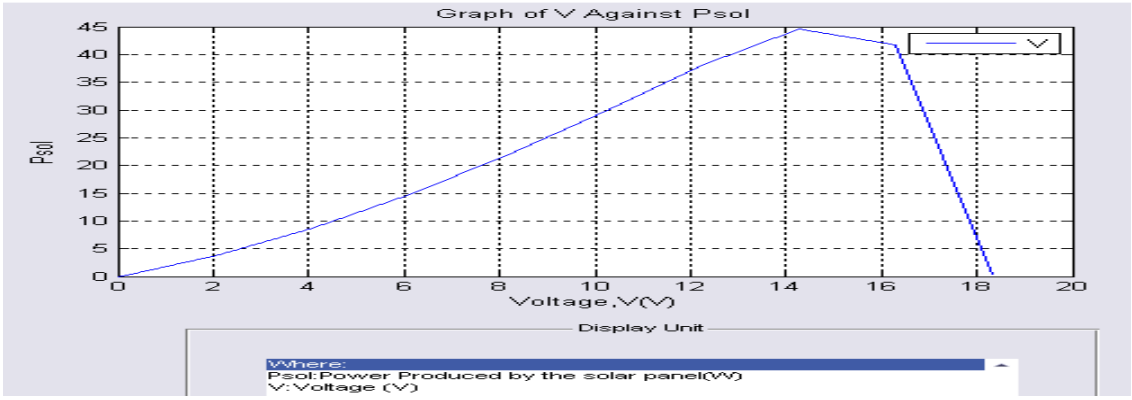

Figure15. Psol-V curve for the KC65T by Kyocera at an incident solar radiation of 400W/m^2

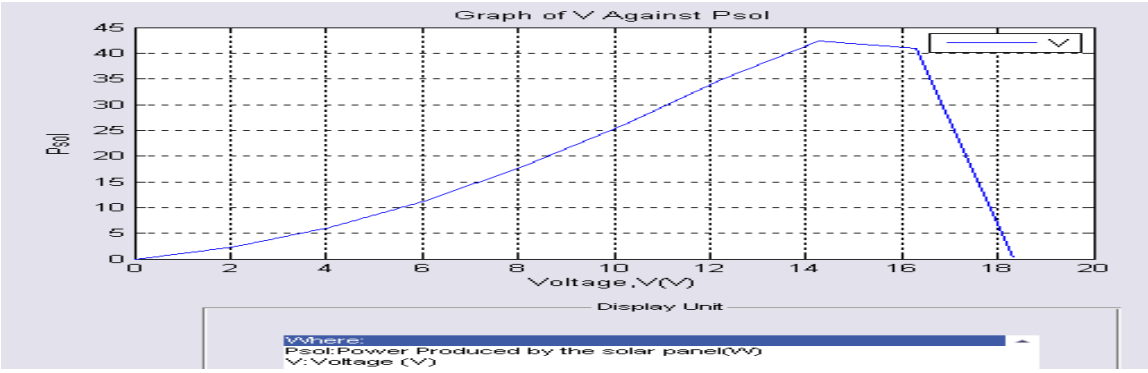

Figure.16. Psol-V curve for the KC65T by Kyocera at an incident solar radiation of 200W/m^2

From the power-voltage graphs of figures 13 – 16 shown above, we note that the power is maximum at a single operating point i.e. at V = 14.2Volts. This is known as the "Maximum Power Point", or **MPP**. If one is to get the most out of their solar cells, it is essential to operate around the MPP. That is to say that in order to get the maximum power output from any solar PV panel, one has to operate at voltages that correspond to the maximum power point, MPP. This voltage is known as the Voltage at maximum power point, $\mathbf{V_{mp}}$ and it is 14.2 volts in this case. From figs 8 – 10, we can deduce the current at maximum power (**MPP**), $\mathbf{I_{mp}}$ i.e. current at $\mathbf{V_{mp}}$ (I at V= 14.2 volts). Table 3 below summarizes the power at MPP, V_{mp} and $\mathbf{I_{mp}}$ at different solar radiation.

Table 3: Summary of the power at MPP and the V_{mp} at different solar radiation

G_T	MPP power	V_{mp}	I_{mp}
1000	51	14.2	3.6
800	49	14.2	3.4
400	44.5	14.2	3.15
200	42	14.2	2.95

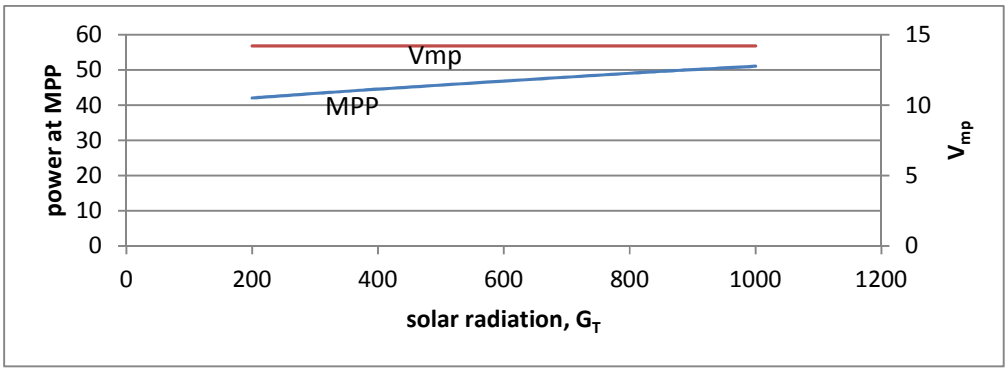

Figure17. Graph of Power at MPP and V_{mp} against G_T

We can also deduce from the graph of fig. 17 that the power at **MPP** increases with increasing solar insolation while the $\mathbf{V_{mp}}$ remains constant at 14.2 volts irrespective of the level of incident solar insolation. This finding suggests that for any particular solar PV panel model, maximum power can be obtained at a particular voltage (14.2 volts in this case), when working at any given solar insolation level. Also, from fig. 18 below, it is observed that $\mathbf{I_{mp}}$ increases with increasing solar insolation.

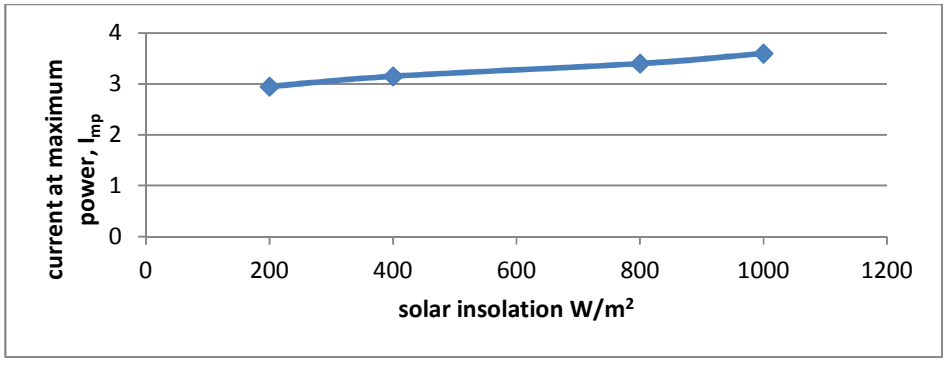

Figure18. Graph of I_{mp} against G_T

4. Conclusions

The aim of this research is to develop a computer model for a photovoltaic powered refrigeration system. This paper also provided a means of choosing the size of the battery such that the refrigerator load is always met, when the solar radiation is unavailable (a period of 12 consecutive hours as used in this paper).

The system (computer model) consists of a solar PV panel, a battery, an inverter, a controller and a vapor compression refrigeration system. A MATLAB model has been developed to simulate the system performance and the simulation can be run using different solar PV panels.

When using solar PV panels, one has to be able to get the maximum power output available from the solar panel. In order to produce maximum power, a person using the KT65T by Kyocera has to operate the system at a voltage of 14.2V which has been found to be the voltage at maximum power, $\mathbf{V_{mp}}$ of the system. Operating the system at any voltage lower than or greater than this does not utilize the potentials of the PV panel thoroughly and thus reduces the efficiency of the system. We have also seen that the $\mathbf{V_{mp}}$ is not affected by the level of solar radiation available. The current at maximum power, $\mathbf{I_{mp}}$ has been observed to increase with increasing solar radiation.

Consequently, one can analyze the system's performance using any PV panel, with the aid of the computer model developed in this paper.

References

Bansal, N.K., Blumenberg, J., Kavasch, H.J., & Roettinger, T. (1997). *Performance testing and evaluation of solid absorption solar cooling unit*, Solar Energy, **61**, 2, 127-140.

BJ Power Co. Ltd. (2009). *Products specification catalogue*, http://www.bjpower.co.kr.BP Solar Corporation., 2008, *Products Data Sheet*, www.bpsolar.com.

Kim, D.S., & Infante Ferreira, C.A. (2008). *Solar refrigeration options – a state-of-the-art review*, international journal of refrigeration (31) 3–15.

Duffle, J.A., & Beckman, W.A. (1991). *Solar Engineering of Solar Processes*, John Wiley & Sons, Inc.

Eckstein, J. (1990). *Detailed Modeling of Photovoltaic System Component*, M.S. Thesis, University of Wisconsin – Madison.

Shan, K.W. **(**2000). *Handbook of air conditioning and refrigeration*, McGraw-Hill.

Kribus, A. (2002). *Thermal integral micro-cogeneration systems for solar and conventional use. Journal of Solar Energy Engineering. 124, 189–197.*

Kyocera Solar, Inc. (2009). *Products specification catalogue*, http://www.kyocerasolar.com

Iloeje, O.C. (1977). *Parametric effects on the performance of a solar powered solid absorption refrigerator*, Solar Energy, **40**(3), 191-195.

McConkey, A. (2003). *Applied Thermodynamics for Engineering Technologists-5th ed.*, Pearson Education Limited.

Townsend, T.U. (1989). *A Method for Estimating the Long-Term Performance of Direct-Coupled Photovoltaic Systems*, M.S. Thesis, University of Wisconsin –Madison.

Worsøe-Schmidt, P. (1983). *Solar refrigeration for developing countries using a solid absorption cycle*, International Journal on Ambient Energy, **(4)** 115-123.

Zekai. S. (2008). *Solar Energy Fundamentals and Modeling Techniques*, Springer-Verlag London Limited.